Effects of column imperfections on capacity of steel frames in variable loading

Terence Ma[1], Lei Xu[1]

[1]Department of Civil and Environmental Engineering, University of Waterloo, 200 University Avenue West, Waterloo, ON., N2L 3G1, Canada

Corresponding Author:
Lei Xu, University of Waterloo
200 University Avenue West
Waterloo, ON. N2L 3G1
Tel: (519) 888-4567 x36882
Email: lxu@uwaterloo.ca

Abstract

The presence of column initial imperfections in a steel frame can increase deflections and decrease its load carrying capacity. A method is proposed for evaluating the lateral stiffness, inter-storey displacement and deflected column shapes in a semi-braced, semi-rigidly connected planar storey frame subjected to gravity loading and column initial imperfections. An equation is proposed for calculating the inter-storey displacement, which contains the notional load associated with out-of-plumbness imperfections, in addition to a new notional load term associated with out-of-straightness imperfections. Additionally, when the lateral stiffness calculated by the proposed method diminishes, the frame is considered unstable. Different gravity loading scenarios can exist that equally result in the various criteria of capacity being reached defined as either instability, the maximum permissible deflection associated with structural integrity, or the onset of yielding in columns. The proposed method extends the variable loading approach to identify the worst- and best-case scenarios of gravity loading for this to occur. Unlike traditional proportional loading analyses, loads are varied independently of each other in the variable loading approach. Numerical models for the frame subjected to variable loading with accounting for the presence of column initial imperfections are established. It is demonstrated that although the presence of column initial imperfections does not affect the buckling loads of frames, it increases deflections and can significantly reduce the capacity even if the frames are constructed within the allowable tolerances for initial imperfections.

Keywords: notional load; semi-braced; steel frame; lateral stability; variable loading; initial imperfections

1 Introduction

The fabrication and construction process always results in geometrical imperfections in steel members and frames, such as out-of-plumbness and out-of-straightness [1]. The imperfections can compromise the strength of a steel frame by introducing second-order effects and increasing deflections. The consequences of column failures in structures as a result of second-order effects can be catastrophic if the second-order effects are not properly accounted for. It is therefore necessary to develop reliable tools for estimating and assessing the structural integrity of steel frames subjected to gravity loading in consideration for the imperfections.

Presented in this paper is a new methodology for calculating the lateral deflection, inter-storey displacement, and assessing the lateral stability of a semi-braced storey frame subjected to gravity loading with consideration of column initial imperfections. In using the proposed method, the deflection and internal bending moment of the columns in a storey frame can be calculated directly. Both the P-Δ effect arising from out-of-plumbness imperfections and P-δ effect arising from out-of-straightness imperfections are considered. In practice, accounting for the effects of imperfections involves either directly modelling the imperfections in a second-order elastic analysis, or laterally applying a fictitious notional load via the notional load method [1]. It is demonstrated that this notional method can also be applied in the proposed method and yields identical results to directly modelling the imperfections. As the original notional loading method only accounts for out-of-plumbness imperfections [1], a new notional load associated with out-of-straightness imperfections is also proposed based on the derivation of the inter-storey displacement equation. A new minimization problem is also proposed for the determination of the worst- and best-case combinations of variable gravity loads and the corresponding capacities causing any of the following failure modes: instability, a maximum permissible deflection or

inter-storey displacement, or the onset of yielding in the columns. Although the buckling load is not affected by initial imperfections, a frame containing imperfections can deform excessively and yield before the buckling load is reached [2]. The effects of column imperfections on frame deflections and the application of the proposed minimization problem are demonstrated via numerical examples and validated via finite element analysis. The results show that the consideration of failure via excessive deflection or yielding in columns due to column initial imperfections can significantly reduce the variable loading capacity of the example frame constructed within allowable tolerances. Finally, it is noted that the analysis of multi-storey frames can also be accomplished via decomposition into individual storeys and using the proposed equations.

2 Background

The concept of storey-based stability has been developed since the 1970's. Yura [3] concluded that storey buckling of a frame structure shall occur with all of the columns in a storey buckled in a lateral sway mode simultaneously, and thus the stiffness contribution of each column to the storey stability must be considered. LeMessurier [4] and Lui [5] extended this concept by proposing the use of effective column length factors for each column with considering the interactions between the members of the frame. Aristizabal-Ochoa [6] and Xu [7] each presented methods for evaluating lateral stability in accounting for the second-order effects. Given that the instability of a frame can occur via many different loading scenarios in terms of locations and magnitudes, Xu [7] derived the lateral stiffness of an axially loaded semi-rigid column and proposed a stability equation that accounts for the stiffness interaction among columns in a storey. Then, the determination of the worst case gravity loading scenario causing instability associated with variable gravity loading was subsequently solved using a minimization problem.

The role of initial imperfections in columns was investigated by Clarke and Bridge [8], who identified two types of geometrical imperfections: out-of-plumbness and out-of-straightness. Out-of-plumbness refers to the lateral eccentricity between the top and bottom ends of a column, whereas out-of-straightness refers to the curvature of a column resulting from the hot-rolling process [8]. Column initial imperfections can be accounted for in analysis either by direct modelling, as permitted in standards such as the CSA-S16 [9], or through use of the notional load method, which simulates the effects of column out-of-plumbness by applying a fictitious lateral load at the top of each storey of a frame equal to a fraction of the total gravity load [1]. Notional loads have been adopted in the design standards of many countries in the last three decades, and are still used to date [9-12]. However, out-of-straightness imperfections are not considered in the original notional load method since they are typically considered empirically in other design equations [1]. In this paper an equation for computing the inter-storey displacement is proposed, and a new notional load associated with the out-of-straightness imperfection is presented. The proposed method yields identical results of the inter-storey displacement regardless of whether the column imperfections are directly modelled or replaced by the notional loads. As notional loads are applied laterally, the proposed method can further be applied towards considering the effects of lateral loads on the deformations of semi-braced frames as well. Finally, the proposed method presents the modeling of a new minimization problem for determining the critical load scenarios in terms of locations and magnitudes causing lateral instability or satisfying other failure criteria.

It is also noted that the proposed storey-based deformation and lateral stiffness equations can be applied to analyze steel frames containing multiple storeys via the storey decomposition method proposed in [13]. In the storey decomposition method, frames can be decomposed into individual

storeys which are analyzed separately, with lateral stiffness calculated via the proposed storey-based stability method. Although the method proposed in [13] does not consider the presence of initial column imperfections, the storey-based lateral stiffness equation proposed in this study can be used in place of the one originally presented.

3 Deformation and Stability of a Semi-Braced Semi-Rigid Frame

Consider the semi-braced planar storey frame with n bays shown in Fig. (1). The frame is subjected to gravity loads, P_i, and the initial out-of-plumbness and out-of-straightness imperfections shown using the symbols Δ_0 and δ_0, respectively. K_b is the total lateral stiffness provided by additional lateral bracing. Note that the frame is unbraced when $K_b = 0$ and fully braced when $K_b = \infty$. Let the indices i and j correspond to the numbering of the columns and beams, respectively. Similarly, the subscripts c and b correspond to columns and beams, respectively. The elastic modulus, moment of inertia and length of each member are E, I, and L, respectively.

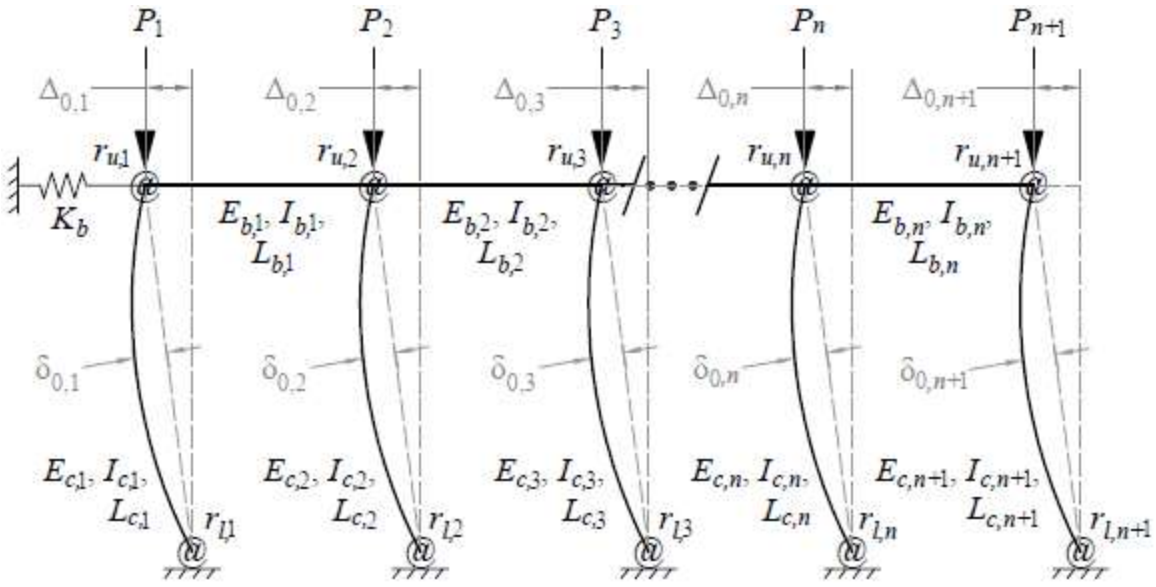

Figure 1 – Semi-braced storey frame subjected to gravity loading and initial imperfections

All connections are generalized as rotational springs, and the column lower and upper end fixity factors are r_l and r_u, respectively. The end fixity factors were originally defined by Monforton and Wu [15] and are shown in Eqs. (1).

$$r_{u,i} = \frac{1}{1 + 3E_{c,i}I_{c,i} / R_{u,i}L_{c,i}}; \quad R_{u,i} = \sum_{j_u=1}^{m_u} R_{i,j_u} \tag{1a}$$

$$r_{l,i} = \frac{1}{1 + 3E_{c,i}I_{c,i} / R_{l,i}L_{c,i}}; \quad R_{u,i} = \sum_{j_l=1}^{m_l} R_{i,j_l} \tag{1b}$$

where R_u and R_l are the rotational stiffness of the upper and lower end connections of the column, respectively. m_u and m_l refer to the number of beams connected to the upper and lower ends of column i, respectively. The end fixity factors are defined such at r = 0 represents a pinned-end connection, and r = 1 represents a fixed-end connection. Intermediate values of r between zero and unity can be used to represent semi-rigid connections. The rotational restraint provided by beam j to column i at the corresponding end, $R_{i,j}$, can be calculated using Eq. (2).

$$R_{i,j} = \frac{6E_{b,j}I_{b,j}r_{N,j}}{L_{b,j}}\left[\frac{2 + v_{FN}r_{F,j}}{4 - r_{N,j}r_{F,j}}\right] \tag{2}$$

where $r_{N,j}$ and $r_{F,j}$ are the end-fixity factors for the near and far ends of beam j connected to column i, and v_{FN} is the ratio of rotation of the far end connection of the beam, θ_F, to the rotation of the near end connection of the beam, θ_N. According to Xu [7], during buckling the ratio v_{FN} depends on the buckling mode of the frame, which is unknown until buckling occurs and needs to be assumed. Xu and Liu [16] demonstrated that accurate estimations of results can be obtained by assuming the case of asymmetric buckling, v_{FN} = 1, for semi-braced partially restrained frames.

3.1 Effect of Imperfections

Each column in the frame is subjected to the prescribed imperfections shown in Fig. (2) [14]. δ_0 corresponds to a sinusoidal out-of-straightness imperfection, and Δ_0 corresponds to an out-of-

plumbness imperfection. The diagram on the right of Fig. (2) depicts the deformation and forces acting on a single column in the state of equilibrium.

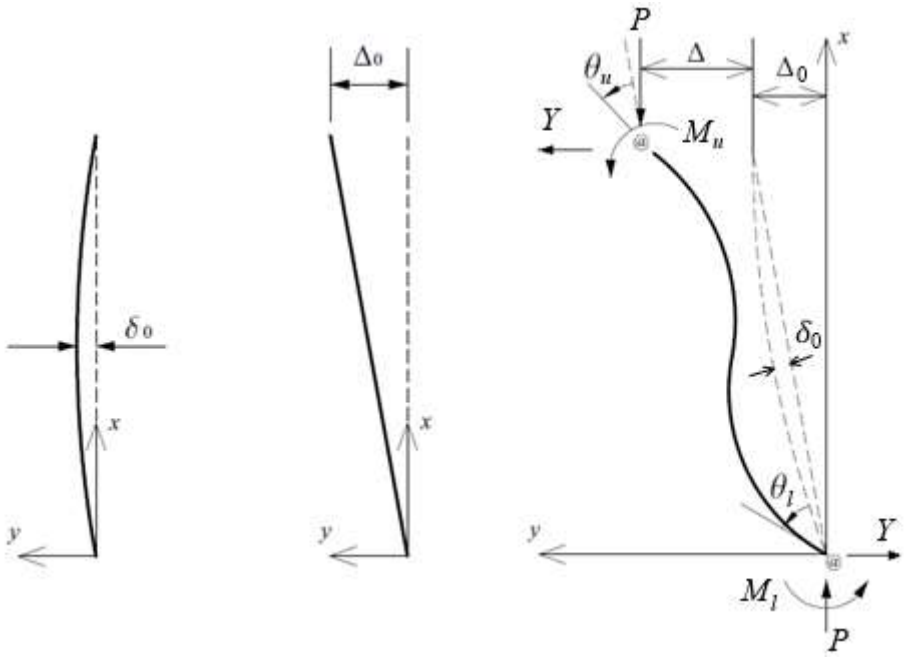

Figure 2 – Schematic of initial imperfections in individual columns [14]

The end moments M_u and M_l, are shown in the positive counter-clockwise convention but act in the opposite direction. Let Y be the transverse force acting at the ends of the column. The imperfection function related to out-of-straightness of the column, $y_1(x)$, is assumed to be a sinusoidal function given in Eq. (3) [2].

$$y_1 = \delta_0 \sin\frac{\pi x}{L} \tag{3}$$

The imperfection function related to out-of-plumbness of the column, $y_2(x)$, is assumed to be linearly varying, as shown in Eq. (4) [2].

$$y_2 = \frac{\Delta_0}{L} x \tag{4}$$

For purposes of simplicity, the imperfect length of the column is approximated such that the upper end matches the height of the storey, which is valid for small deformations. The end moments M_u and M_l relate to the additional end rotations, θ_l and θ_u, in Eq. (5).

$$M_u = R_u\theta_u; \quad M_l = R_l\theta_l \tag{5}$$

Taking moments about the base of the column thus gives the following relationship between the end rotations in Eq. (6).

$$\theta_l R_l + \theta_u R_u = YL + P(\Delta + \Delta_0) \tag{6}$$

The method of sections was utilized to determine the governing differential equation in Eq. (7).

$$M_{\text{int}} = EI\frac{d^2y}{dx^2} = \theta_l R_l - P(y + y_1 + y_2) - Yx \tag{7}$$

Where y is the additional deflection to the initially imperfect shape. Note that in using the Euler-Bernoulli equation, the shear and axial deformations are assumed to be neglected in the analysis. Solving the differential equation in Eq. (7) results in the final deformed shape and bending moment function in Eqs. (8).

$$y(x) = C_1\cos\left(\frac{\phi}{L}x\right) + C_2\sin\left(\frac{\phi}{L}x\right) + \frac{M_l}{P} - \frac{\phi^2\delta_0\sin(\pi x/L)}{\phi^2 - \pi^2} - \frac{\Delta_0}{L}x - \frac{Y}{P}x \tag{8a}$$

$$y'(x) = C_2\frac{\phi}{L}\cos\left(\frac{\phi}{L}x\right) - C_1\frac{\phi}{L}\sin\left(\frac{\phi}{L}x\right) - \frac{\phi^2\delta_0(\pi/L)\cos(\pi x/L)}{\phi^2 - \pi^2} - \frac{\Delta_0}{L} - \frac{Y}{P} \tag{8b}$$

$$M(x) = -P\left(C_1\cos\left(\frac{\phi}{L}x\right) + C_2\sin\left(\frac{\phi}{L}x\right) + \frac{\delta_0\pi^2}{\pi^2 - \phi^2}\sin\left(\frac{\pi}{L}x\right)\right) \tag{8c}$$

where $\phi = L\sqrt{P/EI}$ is the axial load coefficient [7], and C_1 and C_2 are integration constants. There are four boundary conditions to this problem, listed in Eqs. (9).

$$y(0) = 0 \tag{9a}$$

$$y(L) = \Delta \tag{9b}$$

$$y'(0) = \theta_l \tag{9c}$$

$$y'(L) = \theta_u \tag{9d}$$

Solving the system of five equations comprising of Eq. (6) and Eqs. (9) and isolating for Δ results in the deflection of the upper end of the column, which is the inter-storey displacement given in Eq. (10a). The solutions for C_1, C_2 are also provided in Eqs. (10b) and (10c).

$$\Delta = \left[Y + \frac{P\Delta_0}{L} + \frac{P\delta_0}{L}\chi\right] \Big/ \left[\frac{12EI}{L^3}\beta\right] \tag{10a}$$

$$C_1 = \frac{1}{D_c}\left[\frac{\delta_0 \pi}{(\pi^2 - \phi^2)}\varepsilon_{1,1} + \Delta\varepsilon_{1,2}\right] \tag{10b}$$

$$C_2 = \frac{1}{D_c}\left[\frac{\delta_0 \pi}{(\pi^2 - \phi^2)}\varepsilon_{2,1} + \Delta\varepsilon_{2,2}\right] \tag{10c}$$

Where β is the same stiffness modification factor derived in Xu (2001) given in Eq. (11a), and χ is the out-of-plumbness influence coefficient given in Eq. (11e). Eqs. (11f) through (11j) contain the terms used to compute the constants C_1 and C_2.

$$\beta = \frac{\phi^3}{12}\frac{a_1\phi\cos\phi + a_2\sin\phi}{18r_l r_u - a_3\cos\phi + (a_1 - a_2)\phi\sin\phi} \tag{11a}$$

$$a_1 = 3[r_l(1-r_u) + r_u(1-r_l)] \tag{11b}$$

$$a_2 = 9r_l r_u - (1-r_l)(1-r_u)\phi^2 \tag{11c}$$

$$a_3 = 18r_l r_u + a_1\phi^2 \tag{11d}$$

$$\chi = \frac{3\phi^3\pi\sin\phi(r_u - r_l)}{(\pi^2 - \phi^2)(18r_l r_u - a_3\cos\phi + (a_1 - a_2)\phi\sin\phi)} \tag{11e}$$

$$\varepsilon_{1,1} = 3r_l\phi\left(3r_u\phi(1+\cos\phi) - 6r_u\sin\phi - (1-r_u)\phi^2\sin\phi\right) \tag{11f}$$

$$\varepsilon_{2,1} = \phi\left[9r_u r_l\phi\sin\phi - 18r_u r_l(1-\cos\phi) - 3\phi^2\left(r_u(1-r_l) - r_l(1-r_u)\cos\phi\right)\right] \tag{11g}$$

$$\varepsilon_{1,2} = -9r_u r_l(1-\cos\phi) - 3r_l(1-r_u)\phi\sin\phi \tag{11h}$$

$$\varepsilon_{2,2} = 9r_u r_l\sin\phi + 3\phi\left(r_u(1-r_l) + r_l(1-r_u)\cos\phi\right) \tag{11i}$$

$$D_C = 18r_l r_u - a_3\cos\phi + (a_1 - a_2)\phi\sin\phi \tag{11j}$$

Finally, note that the end rotations θ_l and θ_u can be obtained by substituting the values of C_1 and C_2 into Eq. (8b). The denominator in Eq. (10a) is independent of the imperfections, and is in fact identical to the lateral stiffness of the column derived by Xu [7]. It also represents the tangent lateral stiffness of the column ($\partial\Delta/\partial Y$), hereafter denoted as S_T via Eq. (12).

$$S_T = \frac{\partial\Delta}{\partial Y} = \frac{12EI}{L^3}\beta \tag{12}$$

The numerator in Eq. (10a) shows the effect of the transverse force, Y, and imperfections Δ_0 and δ_0 on the inter-storey displacement. In particular, it is noted that the $P\Delta_0/L$ term is equivalent to the notional load [1] for out-of-straightness imperfections, acting in the same direction as Y. It is easy to see that if the out-of-plumbness imperfection was replaced in the derivation by an equivalent notional load $Y' = P\Delta_0/L$ acting coincidentally with Y, Eq. (10a) will remain

unchanged. As such, the application of the notional load method [1] for the out-of-plumbness imperfections produces identical results for calculating the inter-storey displacement. The term containing δ_0 acts in a similar manner as the Δ_0 term but is related to the out-of-straightness rather than the out-of-plumbness. As such, it is hereafter referred to as the notional load accounting for out-of-straightness imperfections. It can be positive or negative depending on whether the column bows in the same direction as Δ, as well as the relative values of the end fixity factors, which affect the value of χ. The maximum deflection can be obtained by evaluating the deflected shape via summing $y_{1,} y_2$ and y in Eq. (13) and then discretizing over the lengths of the columns.

$$\delta(x) = y(x) + y_1(x) + y_2(x) \tag{13}$$

Note that in the absence of out-of-straightness imperfections, the maximum deflection of the columns is at the upper end. Eq. (10a) is applicable for compressive axial loads less than the column rotational buckling load, shown in Eq. (14) [17].

$$0 \le P_i < P_{u,i} = \frac{\pi^2 E_{c,i} I_{c,i}}{(K_i L_{c,i})^2}; \quad K_i = \frac{\pi}{\phi_{u,i}} \tag{14}$$

where $P_{u,i}$ is the rotational buckling load of column i, K_i is the equivalent column length factor, and $\phi_{u,i}$ is the critical load factor corresponding to the minimum value of ϕ resulting in a zero denominator of β in Eq. (11a). An approximation of K is given in Eq. (15), with a maximum error of less than 4%, which subsequently results in up to 8% error in the value of P_u [17].

$$K_i = \sqrt{\frac{\left(\pi^2 + (6-\pi^2) r_{u,i}\right) \times \left(\pi^2 + (6-\pi^2) r_{l,i}\right)}{\left(\pi^2 + (12-\pi^2) r_{u,i}\right) \times \left(\pi^2 + (12-\pi^2) r_{l,i}\right)}} \tag{15}$$

The general effect of increasing the axial load towards the lateral stiffness of a column, S_T, is illustrated in Fig. (3). Except where $r_l = r_u$, S_T asymptotically approaches negative infinity as P increases towards P_u. Otherwise, for $r_l = r_u$, S_T is discontinuous at P_u and indicates the

occurrence of rotational buckling at $P = P_u$. As the difference between the end fixity factors approaches zero, the dotted curve in Fig. (3) will tend towards the one for the solid line corresponding to the condition where $r_u = r_l$. Beyond N_u, the mathematical value of the lateral stiffness equation is plotted in Fig. (3) but does not bear any physical meaning. Note that for the lean-on condition ($r_u = r_l = 0$) the lateral stiffness converges to a linear equation of the axial load [7].

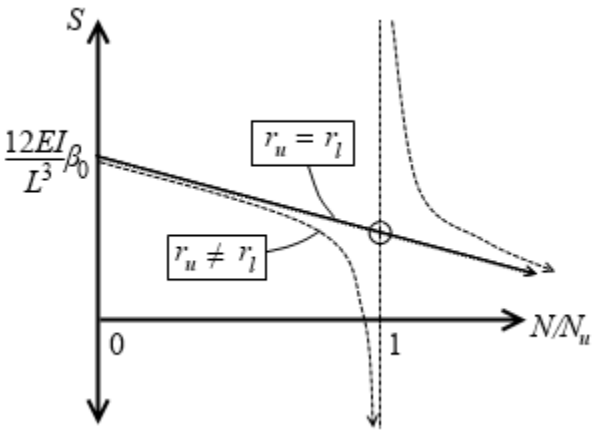

Figure 3 – Generalized plots of tangent stiffness versus axial load

To account for partial yielding and inelastic buckling of the column associated with large axial loads, the elastic modulus can be empirically adjusted using the tangent modulus approach [18]. Assuming that all of the columns in a storey deflect by the same amount, which is valid for rigid floors or roofs located at top of the storey, it can be shown that the deflection of the storey frame in Fig. (1) can be expressed in Eq. (16).

$$\Delta = \sum_{i=1}^{n+1}\left[Y_i + \frac{P_i \Delta_{0,i}}{L_{c,i}} + \frac{P_i \delta_{0,i}}{L_{c,i}} \chi_i \right] \Bigg/ \left[\sum_{i=1}^{n+1} S_{T,i} \right] \tag{16}$$

It is further noted that the sum of lateral forces Y_i experienced by the columns is equal to the total externally applied lateral force at the upper end of the frame, Q, less the lateral bracing force equal to $K_b\Delta$, as shown in Eq. (17).

$$\sum_{i=1}^{n+1} Y_i = Q - K_b \Delta \tag{17}$$

Thus, substituting Eq. (17) into Eq. (16) and rearranging for the inter-storey displacement results in Eq. (18).

$$\Delta = \frac{Q + \sum_{i=1}^{n+1} \left[\frac{P_i \Delta_{0,i}}{L_{c,i}} + \frac{P_i \delta_{0,i}}{L_{c,i}} \chi_i \right]}{\sum_{i=1}^{n+1} S_{T,i} + K_b} \tag{18}$$

Note that $\Delta_{0,i}$ and $\delta_{0,i}$ may be either positive or negative depending on whether they exist in the same or opposite direction as Δ, respectively. If the directions of the imperfections are not known for the individual columns, a conservative estimation of the inter-storey displacement can be attained by summing the absolute values of the imperfection terms in Eq. (18), resulting in the inequality in Eq. (19).

$$\Delta \leq \frac{Q + \sum_{i=1}^{n+1} \left[\frac{P_i}{L_{c,i}} \left| \Delta_{0,i} \right| + \frac{P_i}{L_{c,i}} \left| \delta_{0,i} \chi_i \right| \right]}{\sum_{i=1}^{n+1} S_{T,i} + K_b} \tag{19}$$

Let the storey-based lateral stiffness be denoted as ΣS, equal to the denominator in Eq. (18) and repeated in Eq. (20).

$$\Sigma S = \sum_{i=1}^{n+1} S_{T,i} + K_b \tag{20}$$

The storey is laterally stable when $\Sigma S > 0$, and becomes laterally unstable when $\Sigma S = 0$ since theoretically Δ approaches infinity. This instability condition is identical to the one proposed by Xu [7]. As mentioned previously, Eqs. (19) and (20) can also be used in multi-storey frames when the storeys are analyzed individually according to the decomposition approach presented in [13]. Based on Eq. (20), the buckling load of a frame containing columns with imperfections is

not affected by the imperfections. However, the presence of the imperfections influences the magnitudes of deflections as per Eq. (19). Note that an imperfect column will not reach the elastic buckling load corresponding to $\Sigma S = 0$ in reality because Δ increases asymptotically towards infinity as the axial load approaches the buckling load in Eq. (19). In contrast, for perfect columns, bifurcation of the load-deflection plot occurs when $\Sigma S = 0$ and Δ becomes undefined. Also, the inelastic buckling loads can be estimated via empirical methods, such as the one developed by Yura & Helwig [18], which estimates the tangent elastic modulus according to Eq. (21).

$$E = \tau E_0; \quad \tau = \begin{cases} 1 & ; \quad P/P_y < 1/3 \\ -7.38(P/P_y)\log_{10}(1.176P/P_y) & ; \quad P/P_y \geq 1/3 \end{cases} \tag{21}$$

Where $P_y = Af_y$ is the yielding load, A is the cross-sectional area of the column, and f_y is the yield stress. If this approach is used, then inelastic buckling occurs when the lateral stiffness of the storey in Eq. (20) diminishes to zero with the reductions in Eq. (21) applied. Note, however, that Eq. (21) is independent of the magnitudes of the imperfections and should only be used in standard design cases whereby the imperfections are limited to small magnitudes as stipulated in code requirements. Moreover, Eq. (21) accounts for other causes of inelastic buckling not within the scope of this study, such as the presence of residual stresses.

3.2 Definition of Frame Capacity

The capacity of a frame can be defined in various ways, such as in relation to the deformation due to the presence of imperfections. In practice, the permissible inter-storey displacement, as one of the important design criterion concerning the safety, is often stipulated in design codes and standards, such as in the National Building Code of Canada (NBCC) [19], whereby the inter-storey displacement must not exceed 1.0% to 2.5% of the storey height, depending on the classification of the building. Reaching the permissible inter-storey displacement may be

considered as a mode of failure. Alternatively, the capacity can be considered to be reached when yielding in the columns begins to occur under the elastic analysis (with $E = E_0$). The condition during which onset of yielding occurs in the column is then given in Eq. (22).

$$\left|\frac{P}{A}+\frac{M_{\max}(P)}{S_x}\right| = f_y \tag{22}$$

Where S_x is the section modulus and M_{max} is the maximum internal bending moment defined in Eq. (8c). Although no closed form solution can be obtained for M_{max}, good approximates to M_{max} can be obtained by discretizing Eq. (8c) over x. Finally, note that the maximum column deflection may occur at an intermediate height in a column if out-of-straightness imperfections are present. In cases where the maximum deflection of a column is concerned, such as in the design of columns in elevator shafts, the entire deflected shape of each column can be checked via Eq. (13) to ensure that the maximum deflection does not exceed the permissible limit.

3.3 Example 1 – Parametric Study on the Effects of Imperfections and Bracing Stiffness

A numerical example is provided to demonstrate the use of the proposed method. Consider the semi-braced storey frame shown in Fig. (4), which contains out-of-plumbness and out-of-straightness imperfections. Three parametric analyses were conducted, and the corresponding elastic load-deflection curves obtained from Eq. (10a) were plotted: (1) variation of the initial out-of-plumbness Δ_0 for each column between $L_c/100$ to $L_c/500$, (2) variation of the initial out-of-straightness δ_0 between $-L_c/100$ to $+L_c/100$, and (3) variation of the bracing stiffness K_b between zero and infinity. In each of the analyses, the values of imperfections not being varied were zero, and the bracing stiffness was taken as 10^4 N/m for the first two analyses. Each column was assigned the same value of the imperfections in each case. Note that positive values of δ_0 indicate that the column is bowing towards the left, whereas negative values of δ_0 indicate that the column is bowing towards the right. Also, as some of the values of the imperfections selected

in the analysis exceed the typical values specified in design codes, this investigation also demonstrates what can happen if the imperfections exceed the design limits.

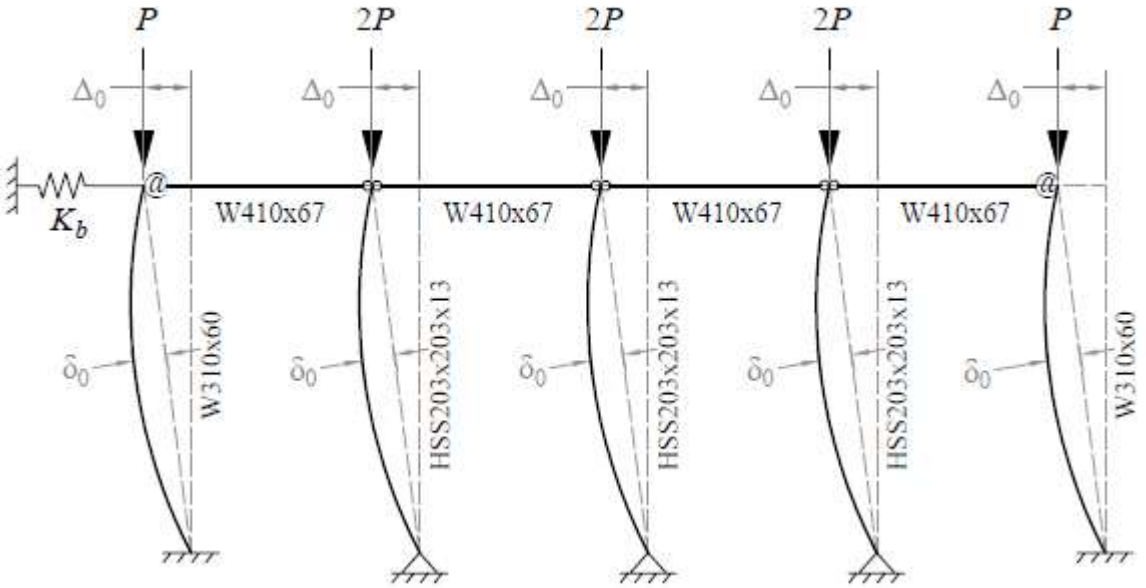

Figure 4 – Four-bay semi-braced steel frame for Example 1

The gravity loads in this example are proportional as shown in Fig. (1), with the interior columns experiencing twice the gravity loads compared to those of the exterior columns. The exterior columns are fixed to the base of the frame (r_I = 1), while the interior columns are pinned to the base of the frame (r_I = 0). The exterior beam-to-column connections are semi-rigid (r_N or r_F = 0.9) and the interior beam-to-column connections are pinned (r_N or r_F = 0), meaning that the three interior columns are lean-on. All of the columns have a length of $L_{c,i}$ = 7.315 m, also equal to the storey height H. The moments of inertia of the exterior and interior columns are 129×10^6 mm^4 and 54.7×10^6 mm^4, respectively. The cross-sectional areas of the exterior and interior columns are 7,610 mm^2 and 9,280 mm^2, respectively. As such, the slenderness ratios of the columns are 32.3 and 95.3 for the exterior and interior columns, respectively. For all beams $L_{b,j}$ = 7.315 m, $I_{b,j}$ = 245×10^6 mm^4, and v_{FN} = 1. Upon investigation, the results of the numerical example are independent of v_{FN} for this example. For the purpose of this example, elastic

behaviour is assumed so E = 200 GPa for all members and is not adjusted based on Eq. (21). Since the interior columns are lean-on they possess zero lateral stiffness in the absence of axial loads. The lateral stiffness of the interior columns with axial loads applied will become negative which signifies that they rely on the lateral support provided by other columns to sustain the applied gravity loads.

3.3.1 Effect of Out-of-Plumbness

The elastic load-deflection curves for the frame subjected to only out-of-plumbness imperfections are plotted in Fig. (5). As out-of-straightness imperfections are not present, the maximum deflection of each column will be at the upper end. The total inter-storey displacement, $\Delta+\Delta_0$, is plotted on the abscissa. For every load-deflection curve the magnitude of P is increased until instability occurs. The load-deflection curve of the frame without considering out-of-plumbness imperfections is also plotted for the reason of comparison.

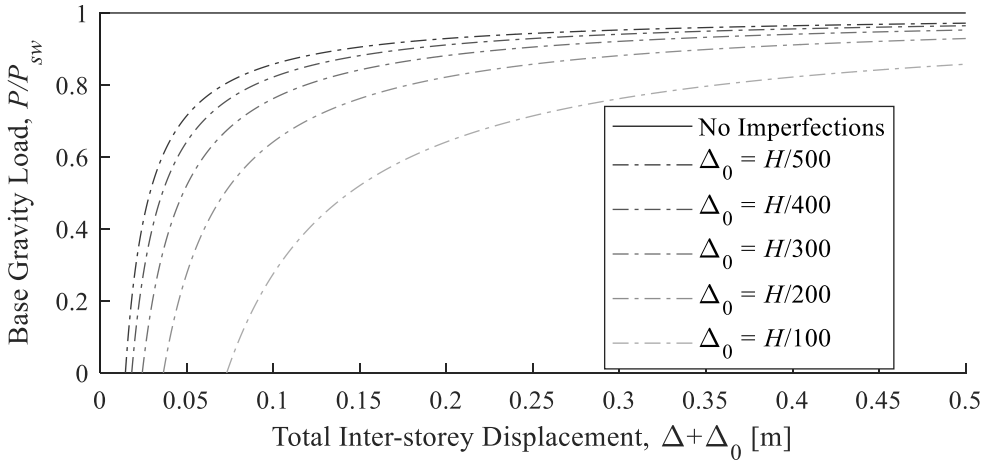

Figure 5 – Load-deflection curve for Example 1 with out-of-plumbness imperfections

In Fig. (5), P_{sw} is the elastic critical sway load of the frame, obtained by solving for the value of P that satisfies $\Sigma S = 0$ with E = 200 GPa. For this example, P_{sw} = 949.7 kN. In the absence of out-of-plumbness imperfections, the deflection is zero until elastic buckling occurs at $P = P_{sw}$.

As the out-of-plumbness imperfections are introduced and increased, the deflection increases for the same applied load and asymptotically approaches infinity as P approaches P_{sw}.

3.3.2 Effect of Out-of-Straightness

The elastic load-deflection curves for the frame subjected to out-of-straightness imperfections are plotted in Fig. (6). In this case, the maximum magnitude of deflection in each column, δ_{max}, was obtained by evaluating Eq. (13) and plotted on the abscissa.

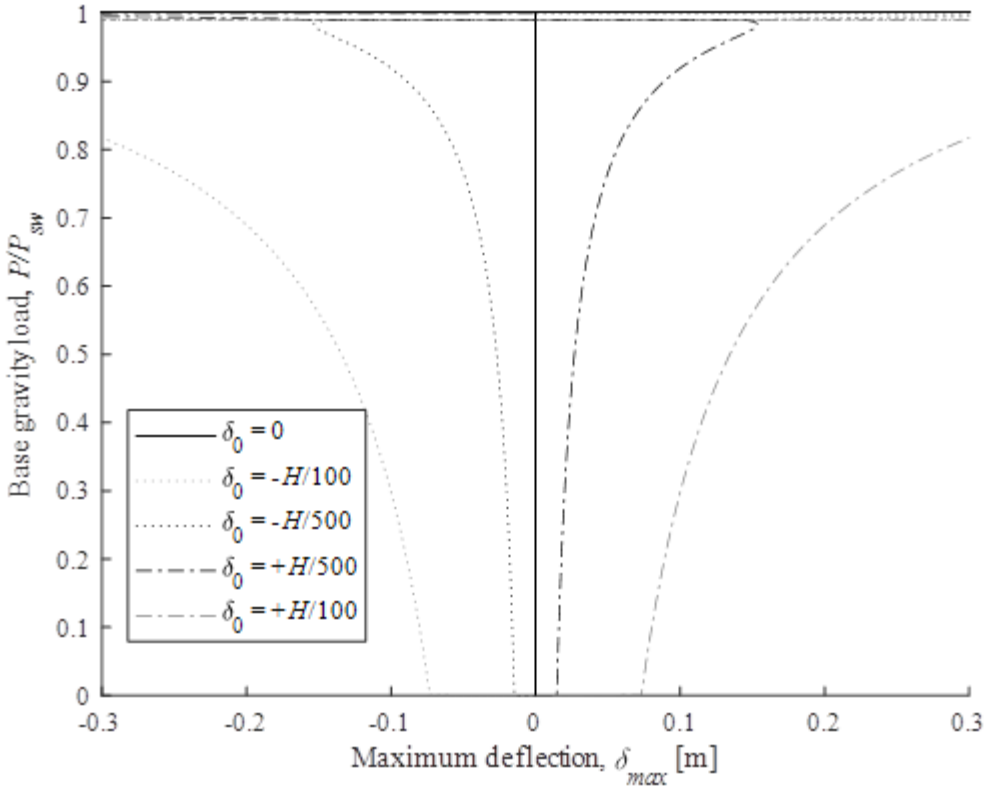

Figure 6 – Load-deflection curve for Example 1 with out-of-straightness imperfections

From Fig. (6) it can be observed that the maximum deflection is increased as the magnitude of the out-of-straightness imperfection is increased. To be clear, if y is measured to the left, then $\delta_0 > 0$ indicates bowing towards the positive y direction and $\delta_0 < 0$ indicates bowing towards the negative y direction. The plot is symmetrical because the frame is symmetrical. For each of the curves, the maximum deflection is initially in the same direction as the initial bowing direction

for low load levels. At these load levels, the maximum deflection in the frame is governed by the deflection at the mid-height of the lean-on columns. However, as the load increases, the upper end of the column moves in the opposite direction. Although the column initially bows outwards it begins to move towards the opposite direction, as indicated by the rounded corners in curves associated with $\delta_0 = \pm H/500$ just before the curves cross the ordinate near $P/P_{sw} \approx 0.98$. The curves cross the ordinate when the deflection of the upper ends of the columns governs the maximum deflection of the frame. The same behaviour occurs for the $\delta_0 = \pm H/100$ curves but at much higher deflections. The inter-storey displacement, Δ, is also plotted in Fig. (7).

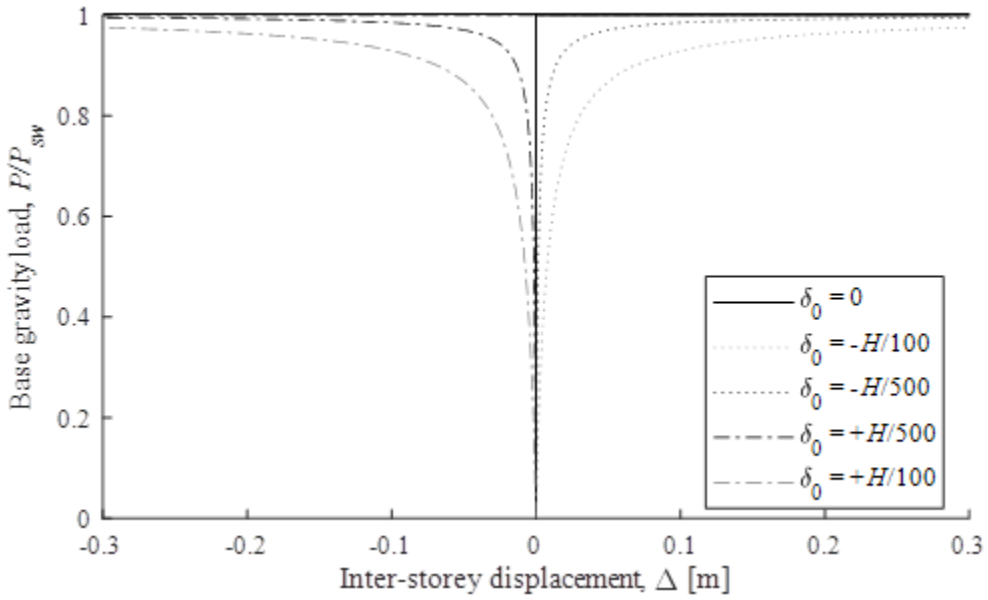

Figure 7 – Inter-storey drift for Example 1 with out-of-straightness imperfections

As discussed previously, the direction of Δ is in the opposite direction to the bowing direction of the initial out-of-straightness imperfection. As the frame is symmetrical, the plot is also symmetrical. Overall, the out-of-straightness imperfections appear to have a comparable effect on the maximum deflection in this example when the values in Fig. (6) are compared to the out-of-plumbness imperfections of the same magnitude from Fig. (5). Also, from comparing Figs. (6) and (7) maximum deflection may not necessarily occur at the upper end of the columns.

3.3.3 Effect of Bracing Stiffness

The value of K_b affects the value of P_{sw}, which is independent of the imperfections and is plotted in Fig. (8). It is noted that K_b also affects the magnitude of deflection, for $P < P_{sw}$.

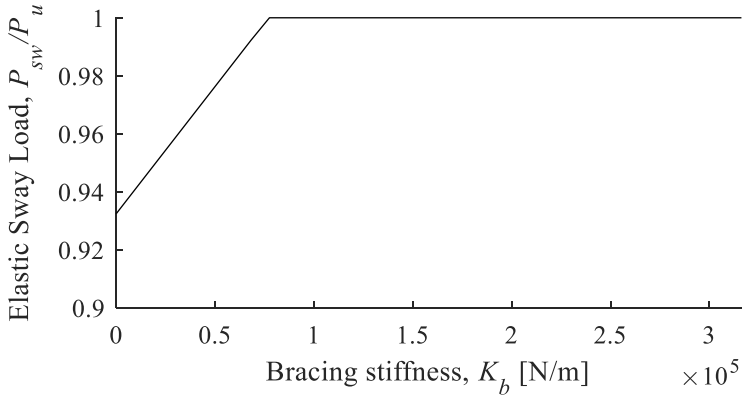

Figure 8 – Load-deflection curve for Example 1 with varying bracing stiffness

From Fig. (8), the elastic sway load varies between a minimum value of P_{sw} = 941 kN to a maximum value of P_u = 1,009 kN, attained with $K_b \geqslant$ 77 kN/m or higher. Thus, for this example if lateral bracing of at least 77 kN/m is provided then the frame can be treated as fully braced. P_u = 1,009 kN corresponds to the rotational buckling of the three identical interior lean-on columns (since the load factor is 2, the rotational buckling loads of the interior columns are each 2,018 kN). Note that if the interior columns were semi-rigidly or rigidly connected then P_{sw} would asymptotically approach P_u with increasing K_b, rather than reaching P_u at a finite value of K_b [20].

3.3.4 Finite Element Modelling

A finite element model was created in ABAQUS [21] to validate the above results using cubic wireframe B23 Euler-Bernoulli (non-shear-deformable) elements in all members. Note that the effect of axial load on the lateral stiffness is considered in using the B23 elements. In all cases, the elastic sway loads obtained in ABAQUS converged to the results of the out-of-plumbness,

out-of-straightness and lateral bracing parametric studies, with a maximum difference of only 0.5%. The differences in the results are attributed to the effect of axial deformations, the use of linear piece-wise segments in ABAQUS to approximate the sine curve in Eq. (3), and the length of the column being assumed to be equal to the height of the storey in the proposed method. The inter-storey displacements and maximum values of *y(x)* (maximum deflection less imperfections) obtained in Figs. (5) and (6), respectively, were also checked in the model via the Nlgeom feature [21] for several cases, shown in Fig. (9). Note that only the values of *y(x)* in Eq. (8a), rather than the deflection *δ(x)* in Eq. (13) were outputted by ABAQUS. In any case, the assessment of accuracy with comparing *y(x)* between the proposed method and ABAQUS is analogous to comparing the deflections. Curves I, II and III correspond to the inter-storey displacement with $\Delta_0 = H/100$, $H/200$ and $H/400$, respectively. Curve IV corresponds to the maximum deflection with $\delta_0 = H/100$.

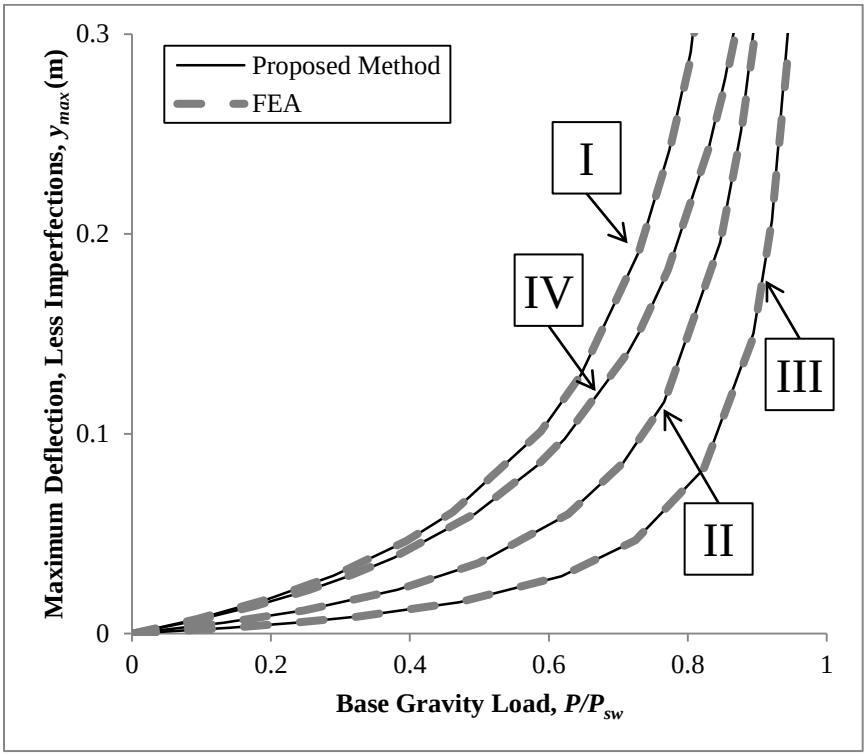

Figure 9 – Comparison of maximum deflections obtained with the proposed method and FEA

The differences between the values computed by the proposed method and FEA were within 1% when the maximum deflection (less imperfections) of the frame was below 0.1 m = *L*/73. The errors increase as the displacement quantities increase, as a result of the small deformations assumption (theoretically, the error tends to infinity at the buckling load as one model will return a finite deflection whereas the other will become unstable). Errors also arise due to the axial deformations of the columns in the finite element model, which are neglected in the proposed method. As such, the proposed method yields accurate results of the maximum deflection.

4 Frame Capacities with Imperfections Subjected to Variable Gravity Loading

The concept of variable loading is a new design philosophy that focuses on identifying the worst or best scenarios of applied loads causing failure of a structure, and abandons the traditional assumption of proportional loading [7]. There are many different combinations of gravity loads that can similarly result in the failure criteria being reached. The assessment of the worst- or best-case scenarios can be formulated as minimization and maximization problems that solve for the minimum or maximum total applied loads, respectively, that would cause the capacity of the frame to be reached [7]. Note that this is conceptually different from what is commonly known as structural optimization, which also employs the use of minimization problems but with a different objective, which would be to minimize the volume of steel the design. As such, it can be used to evaluate the structural capacity in the most extreme cases of loading or determine the maximum possible capacity that a structure can sustain (in other words, it provides an envelope of the capacity). The capacity of the frame can be defined in the following ways: (a) instability (i.e. $\Sigma S = 0$ corresponding to $\Delta = \infty$), as is the case in Xu [7]; (b) excessive inter-storey drift ($\Delta = \Delta^*$, where Δ^* is the permissible inter-storey drift); (c) excessive deflection ($\delta_{max} = \delta^*$, where δ^*

is the permissible deflection based on design requirements); (d) onset of yielding as per Eq. (22); or any other related failure criterion.

Using criterion (a) related to the instability of the frame ($\Sigma S = 0$ corresponding to $\Delta = \infty$) results in a minimization problem identical to that proposed in Xu [7], shown in Eqs. (23), which is independent of the imperfections. However, unlike in [7], Eqs. (23) can now also be used when considering inelastic buckling as the instability criterion via the use of the empirical tangent modulus in Eq. (21).

$$\min \text{ or } \max \sum_{i=1}^{n+1} P_i; \quad \text{subject to:} \tag{23a}$$

$$\Sigma S = \sum_{i=1}^{n+1} \left[\frac{12 E_{c,i} I_{c,i}}{L_{c,i}^{3}} \beta_i \right] + K_b = 0 \tag{23b}$$

$$P_{l,i} \le P_i \le P_{u,i} \quad (i = 1,2,\ldots,n) \tag{23c}$$

where P_i are the variable axial loads, $P_{l,i}$ is the lower bound gravity load which may either be taken as zero or prescribed by the user to account for dead loads, and $P_{u,i}$ is the rotational buckling load of column i. Note that if the stage of design for the structure is sufficiently advanced, the values of $P_{l,i}$ and $P_{u,i}$ may alternatively be prescribed based on the expected ranges of applied loading related to known occupancies. When considering the column imperfections, however, the excessive inter-storey drift, excessive deflection and onset of yielding criteria will usually be reached before instability occurs, and are therefore generally more conservative. The only exception to this is the case of a frame containing columns with $r_u = r_l$ (most commonly, $r_u = r_l = 0$ for lean-on columns), whereby instability can occur suddenly via rotational buckling (as the lateral stiffness of such a column does not asymptotically decrease with applied loading due to the removal discontinuity in Fig. (3), the deflections also do not asymptotically approach infinity). In any case, when considering the alternative criteria, the failure constraint in Eq. (23b)

can be replaced by any one of the capacity criteria, (b) through (d), in Eqs. (24a) through (24c), respectively.

$$\Delta = \frac{Q + \sum_{i=1}^{n+1}\left[\frac{P_i \Delta_{0,i}}{L_{c,i}} + \frac{P_i \delta_{0,i}}{L_{c,i}} \chi_i\right]}{\sum_{i=1}^{n+1} S_{T,i} + K_b} = \Delta^* \tag{24a}$$

$$\delta_{\max} = \max_{x,i}\left(\left|\delta_i(x)\right|\right) = \delta^*; \quad i \in [1, n+1], x \in [0, L_{c,i}] \tag{24b}$$

$$\max_i \left(\left| \frac{P_i}{A_i} + \frac{M_{\max,i}(P_i)}{S_{x,i}} \right| - f_{y,i} \right) = 0; \quad i \in [1, n+1] \tag{24c}$$

where Δ^* or δ^* are chosen based on design considerations. Note that in this case, Δ is the inter-storey displacement, and if out-of-straightness imperfections are considered, Δ may not be the maximum deflection in the storey. In Eq. (24b), δ_{max} is the maximum column deflection and δ^* is the permissible column deflection. δ_{max} can be calculated via discretization of the columns in Eq. (13). In Eq. (24c), the constraint detects the instance where onset of yielding occurs in at least one column in the frame. Note that if Eq. (24c) is adopted, then the elastic modulus should not be reduced via the tangent modulus model. Although theoretically redundant, an additional constraint, $\Sigma S > 0$, may also be added to improve the performance of whatever optimization algorithm is used, as it ensures the immediate elimination of the cases where lateral instability has already occurred. The resulting formulation with considering the alternative failure constraints are presented in Eqs. (25).

$$\min \text{ or } \max \sum_{i=1}^{n+1} P_i; \quad \text{subject to:} \tag{25a}$$

$$\Psi = \Gamma \tag{25b}$$

$$\Sigma S = \sum_{i=1}^{n+1}\left[\frac{12 E_{c,i} I_{c,i}}{L_{c,i}^{\,3}} \beta_i\right] + K_b > 0 \tag{25c}$$

$$P_{1,i} \le P_i \le P_{u,i} \quad (i = 1,2,\ldots,n) \tag{25d}$$

where Ψ is the quantity being evaluated against the corresponding limit, Γ. Eq. (25b) can take the form of the conditions in Eqs. (24), which correspond to criteria (b) through (d), or other failure criteria. Eqs. (23) and (25) can be solved using nonlinear constrained optimization algorithms, such as the GRG Nonlinear algorithm [22]. For complicated minimization problems, the performance of the GRG Nonlinear algorithm can be further improved when multi-start searching is enabled, described in [23]. Finally, it is important to note that in solving Eqs. (23) or (25) for the minimum total loads causing the capacity criteria to be reached, the designer should verify that the total load in the final solution does not exceed the rotational buckling limit of any column. Otherwise, the minimum solution shall be appropriately replaced with the case of loading the column with the lowest rotational buckling load until rotational buckling occurs ($P_i = P_{u,i}$). Such a check is required since the minimization problem cannot in itself identify the rotational buckling scenario.

4.1 Computational Procedure for Frame Stability under Variable Loading

A summary of the procedure that can be followed to analyze frames using the proposed variable loading method is provided below.

1. Determine basic member properties ($L_{c,i}$, $L_{b,i}$, $E_{b,i}$, $I_{c,i}$, $I_{b,i}$) and known or assumed end conditions ($r_{u,i}$, $r_{l,i}$, $r_{N,j}$, $r_{F,j}$). In lieu of better predictions, specify $v_{FN} = 1$ for simplicity. Input the bracing stiffness, K_b.
2. Establish the tangent modulus functions for the columns, $E_{c,i}$, or other empirical models.
3. Specify and calculate the values of $P_{l,i}$ and $P_{u,i}$, respectively. Note that the solution for $P_{u,i}$ may be iterative if the tangent modulus approach is adopted.
4. Select values for the initial imperfections (Δ_0 and δ_0) and applied lateral load, Q, if applicable.

5. Define the capacity criterion from Eq. (23b) or Eqs. (24) and solve the minimization problem defined by Eqs. (23) or Eqs. (25) using a non-linear solver program. The solver should output the worst- or best-case combination of loads resulting in the corresponding failure by minimizing or maximizing the objective functions, respectively.
6. If solving for the worst-case combination of loads via minimizing the objective function, verify that the total load in the final solution does not exceed the rotational buckling limit of any column. Otherwise, replace the minimum solution with the case of rotational buckling in the column with the lowest rotational buckling load.

4.2 Example 2 – Variable Loading Analysis

The applied gravity loads were treated as variables in a reanalysis of the frame in Fig. (4), but with $\Delta_0 = H/500$ and $\delta_0 = -H/1000$ for all columns except for in Section 4.2.5, and $K_b = 10^5$ N/m. Note that the chosen magnitudes of the imperfections correspond to the construction tolerances stipulated in [12]. Variable loading analyses were conducted using Eqs. (23) and (25), and the solutions to each problem are presented in Sections 4.2.1 through 4.2.4. This time, the inelastic behaviour of the columns was modelled using the tangent modulus equation in [18] in Eq. (21). For reference purposes, the first-order stiffness of each column, which is the value of $S_{T,i}$ when in the absence of axial loads, and values for $P_{u,i}$ are given in Table 1. To be clear, the lateral stiffness of the columns will decrease from these values as axial loads are applied. To account for the dead loads on the columns, $P_{l,i}$ = 125 kN for the exterior columns and $P_{l,i}$ = 250 kN for the interior columns. The columns are numbered from left to right.

Table 1 – Column properties in variable gravity loading frame example

Scenario	Col. 1	Col. 2	Col. 3	Col. 4	Col. 5	K_b	Storey
First-order lateral stiffness (kN/m)	530.9	0.0	0.0	0.0	530.9	100.0	**1,162**

Rotational buckling load, P_u (kN)	2,215	1,671	1,671	1,671	2,215	-	-

The properties of the frame to this point are consistent throughout each of the analyses in sections 4.2.1 through 4.2.5. Note that as the interior columns are lean-on, the rotational buckling case needs to be checked when solving for the minimum total load in each of the analyses.

4.2.1 Example 2a – Variable Loading Analysis of Storey Instability

The worst case gravity loading scenario causing instability was obtained by first solving Eqs. (23) and tabulating the results in Table 2a. Note that the analysis in this case is independent of the column imperfections since none of the terms in Eqs. (23) nor the rotational buckling loads of the columns are functions of the column imperfections.

Table 2a – Worst case gravity loading scenario causing instability, as obtained by solving Eqs. (23)

	Col. 1	Col. 2	Col. 3	Col. 4	Col. 5	K_b	Total
Gravity load, P_i (kN)	2,208	250.0	250.0	250.0	125.0	-	**3,083**
P_i/P_u	99.7%	15.0%	15.0%	15.0%	5.7%	-	-
Lateral Stiffness, $S_{T,i}$ (kN/m)	-505.0	-34.2	-34.2	-34.2	511.8	100.0	**0.0**

Apparently, based on the results in Table 2a, the worst case loading scenario occurs when Column 1 is loaded until sway buckling of the frame occurs, with all of the other columns kept at their minimum loads (P_l). However, since the interior columns are lean-on ($r_u = r_l = 0$), the rotational buckling loads must also be checked. The total load of 3,083 kN exceeds that which would be experienced by the frame if one of the interior columns buckles rotationally (at $P_{u,i}$ = 1,671 kN for a total of 2,421 kN in the frame). As such, the minimum solution is replaced by the case of rotational buckling shown in Table 2b.

Table 2b – Corrected worst case gravity loading scenario causing instability

	Col. 1	Col. 2	Col. 3	Col. 4	Col. 5	K_b	Total
Gravity load, P_i (kN)	125.0	1,671	250.0	250.0	125.0	-	**2,421**

P_i/P_u	5.7%	100.0%	15.0%	15.0%	5.7%	-	-
Lateral Stiffness, $S_{T,i}$ (kN/m)	511.8	*N/A**	-34.2	-34.2	511.8	100.0	***N/A****

*Denotes discontinuity in the lateral stiffness equation (Eq. 23b) detected when the rotational buckling load is reached

Note that if the load on Column 2 is swapped with that of either of the identical Columns 3 or 4 instead, then an equivalent scenario will be produced. Therefore, the solution to the minimization problem in Table 2b is not unique. Similarly, the solution to Table 2a is not unique since Columns 1 and 5 are identical and the frame is symmetrical. The maximization problem was also solved to determine the best case loading scenario that would result in instability via Eqs. (23). Once again, the solution to Eqs. (22) is independent of the column imperfections. The resulting best case scenario is shown in Table 3.

Table 3 – Best case gravity loading scenario causing instability

	Col. 1	Col. 2	Col. 3	Col. 4	Col. 5	K_b	Total
Gravity load, P_i (kN)	1,259	1,671	1,671	1,671	1,259	-	**7,530**
P_i/P_u	56.8%	100.0%**	100.0%**	100.0%**	56.8%	-	-
Lateral Stiffness, $S_{T,i}$ (kN/m)	292.6	-228.4	-228.4	-228.4	292.6	100.0	**0.0**

** Denotes a column on the verge of rotational buckling, loaded just slightly below the rotational buckling load

Based on the results, the frame has a maximum capacity of 7,530 kN if loaded in the given configuration. The interior lean-on columns are on the verge of rotational buckling, with lateral stiffness of -228.4 kN/m each, meaning that they rely on the stiffness of other columns to maintain stability. As such, the total axial capacity of the frame ranges largely between 1,671 kN for the worst case and 7,530 kN for the best case when variable loading is considered (for this frame, more than a fourfold increase). This knowledge can be useful for design in that occupancies can be assigned to the bays of the frame in proportion to the loads given in the best case scenario to maximize the capacity.

4.2.2 Example 2b – Variable Loading Analysis: Excessive Inter-storey Displacement

Eqs. (25) was applied to determine the worst and best case loading scenarios resulting in the excessive interstorey displacement criterion in Eq. (24a) being reached. An excessive inter-storey displacement criterion of $\Delta^* = H/100$ was specified, based on the requirements of the NBCC [19]. Once again, the Yura & Helwig [18] tangent modulus model in Eq. (21) was used to account for the reduction in elastic modulus associated with high axial stresses. The corresponding worst case scenario determined by the analysis is shown in Table 4.

Table 4 – Worst case gravity loading scenario causing excessive inter-storey displacement as obtained by solving Eqs. (24)

	Col. 1	Col. 2	Col. 3	Col. 4	Col. 5	K_b	Total
Gravity load, P_i (kN)	2,203	250.0	250.0	250.0	125.0	-	**3,078**
P_i/P_u	99.5%	15.0%	15.0%	15.0%	5.7%	-	-
Lateral Stiffness, $S_{T,i}$ (kN/m)	-422.7	-34.2	-34.2	-34.2	511.8	100.0	**66.1**

Similar to that of the stability analysis in Example 2a, the loading of an exterior column was initially found to govern the worst case failure of the frame via solving the minimization problem. However, the case involving rotational buckling of an interior columns needs to be checked and once again has a lower total load of 2,421 kN, shown in Table 2b. In this case, a minimum total load of 3,078 kN is required to achieve the inter-storey displacement of $H/100$, but instability can occur much earlier via rotational buckling when any of the interior columns reaches P_u = 1,671 kN, corresponding to a total load of 2,421 kN in the frame. As such, the results in Table 4 can be replaced with the rotational buckling scenario in Table 2b, as rotational buckling governs the capacity of the frame in this case. Note that if a lower value of Δ^* was selected then the solution the minimization problem would simply correspond to the same loading pattern with a lower load on either of the external columns. The maximization problem was also solved to determine

the best case loading scenario that would result in excessive inter-storey displacement via Eq. (24a). The resulting best case scenario is shown in Table 5.

Table 5 – Best case gravity loading scenario causing excessive inter-storey displacement

	Col. 1	Col. 2	Col. 3	Col. 4	Col. 5	K_b	Total
Gravity load, P_i (kN)	903.3	1,671	1,671	1,671	903.3	-	**6,819**
P_i/P_u	40.8%	100.0%**	100.0%**	100.0%**	40.8%	-	-
Lateral Stiffness, $S_{T,i}$ (kN/m)	391.2	-228.4	-228.4	-228.4	391.2	100.0	**197.1**

** Denotes a column on the verge of rotational buckling, loaded just slightly below the rotational buckling load

Based on the results, the frame has a maximum capacity of 6,819 kN if the maximum permissible inter-storey displacement of $H/100$ is introduced. This is much lower (-9.4%) than the maximum capacity if only stability is concerned. In this scenario, the frame is still stable with a limited lateral stiffness of 197.1 kN/m. The exterior columns provide lateral stiffness such that the interior columns can sustain the applied loads while maintaining the stability of the frame. Similar to the case of Table 3, the interior columns are loaded to the verge of rotational buckling. Upon investigation, loading of the interior columns was found to generally result in a smaller decrease to the lateral stiffness than the loading of the exterior columns. As such, the best case scenario involves loading the interior columns as much as possible, and then loading onto the exterior columns as well until the permissible inter-storey displacement is reached. Overall, the maximum capacity of the frame has been significantly reduced as a result of considering the imperfections along with the maximum deflection criterion.

4.2.3 Example 2c – Variable Loading Analysis: Excessive Maximum Deflection

The minimization and maximization problems in Eqs. (25) were also solved using the permissible maximum deflection constraint in Eq. (24b) with a permissible deflection of $\delta^* = H/100$. The corresponding worst case scenario determined by the analysis is shown in Table 6.

Table 6 – Worst case gravity loading scenario causing excessive deflections

	Col. 1	Col. 2	Col. 3	Col. 4	Col. 5	K_b	Total
Gravity load, P_i (kN)	125.0	250.0	250.0	1,592	125.0	-	**2,342**
δ_{max} (mm)	20.3	20.3	20.3	73.2	20.3	-	-
Lateral Stiffness, $S_{T,i}$ (kN/m)	511.8	-34.2	-34.2	-217.6	511.8	100.0	**837.5**

Based on the results, Column 4 deflects excessively when only P_4 = 1,592 kN of load is applied, but the frame is still stable. Since the interior columns are identical, the same deflection occurs when either Columns 2 or 3 are loaded by the same amount instead. This failure criterion corresponds to a significantly lower minimum capacity of the frame compared to the instability criterion (a reduction of 3.3%). Note that rotational buckling is not imminent, since the total load does not exceed any of the rotational buckling loads of the columns. The maximization problem was also solved, and the results are presented in Table 7.

Table 7 – Best case gravity loading scenario causing excessive deflections

	Col. 1	Col. 2	Col. 3	Col. 4	Col. 5	K_b	Total
Gravity load, P_i (kN)	859.8	1,611	1,611	1,611	859.8	-	**6,552**
δ_{max} (mm)	73.2	73.2	73.2	73.2	73.2	-	-
Lateral Stiffness, $S_{T,i}$ (kN/m)	398.4	-220.2	-220.2	-220.2	398.4	100.0	**246.8**

Based on the results, the maximum case consists of all columns at the permissible deflection limit of $H/100$, and the frame is still stable. The total load is 6,552 kN and corresponds to a 13.0% reduction in the total load corresponding to the permissible deflection compared to the instability problem. Note that in this scenario the maximum deflections of the exterior columns are found at the upper end where $\delta = \Delta+\Delta_0$. The load causing this is lower than that reported in Table 5, in which the maximum deflections in the interior columns do not satisfy the maximum permissible deflection criterion.

4.2.4 Example 2d – Variable Loading Analysis: Onset of Yielding Criterion

The minimization and maximization problems in Eqs. (25) were also solved using the onset of yielding constraint in Eq. (24c). In this case, since the onset of yielding defines the capacity, elastic analysis is assumed with $E = E_0 = 200$ GPa for all members. As such, the empirical tangent modulus model no longer applies and the elastic rotational buckling loads of the columns become $P_u = 14{,}368$ kN for the exterior columns and $P_u = 2{,}018$ kN for the interior columns. The solution to the minimization problem is given in Table 8.

Table 8 – Worst case gravity loading scenario causing onset of yielding

	Col. 1	Col. 2	Col. 3	Col. 4	Col. 5	K_b	Total
Gravity load, P_i (kN)	125.0	250.0	1,729	250.0	125.0	-	**2,479**
f/f_y	9.1%	8.8%	100%	8.8%	9.1%	-	-
Lateral Stiffness, $S_{T,i}$ (kN/m)	511.8	-34.2	-236.4	-34..2	511.8	100.0	**818.8**

In Table 8, f/f_y is the stress utilization ratio, where f is the maximum stress in the column and f_y is the yield stress of 350 MPa. Based on the solution in Table 8, the onset of yielding via Eq. (24c) occurs if one of the interior columns is loaded to 1,729 kN which is less than the corresponding elastic rotational buckling load of 2,018 kN. Note that the load of 1,729 kN is slightly higher than the rotational buckling load obtained using the tangent modulus model with considering inelastic buckling, which is conservative. In any case, a further investigation reveals that for lean-on columns, the integration constants C_1 and C_2 in Eq. (10b) and (10c) respectively become zero, and the corresponding bending moment functions therefore become independent of the inter-storey displacement. As such, the stresses in the interior columns are independent of the loads in the other columns. The solution is not unique, since the loading of any interior column to 1,729 kN will therefore cause the onset of yielding. Note that the stresses in the exterior columns are functions of the inter-storey displacement via Eqs. (10b) and (10c), and are subsequently influenced by the load in Column 3, resulting in a 9.1% stress utilization ratio,

corresponding to a maximum of 31.9 MPa stress in the columns. Nevertheless, the minimum solution is largely governed by the loading of any single interior column, and a total load of 2,479 kN. Although this value is higher than that obtained via the more conservative inelastic analysis, it is still 10.4% lower than the load required to cause instability via rotational buckling of an interior column with all other columns kept at minimum loads ($P_{l,i}$) in the elastic analysis ($P_{u,i}$ = 2,018 kN for one interior column, for a total applied gravity load of 2,768 kN in the frame). Anyway, the solution to the maximization problem is given in Table 9.

Table 9 – Best case gravity loading scenario causing onset of yielding

	Col. 1	Col. 2	Col. 3	Col. 4	Col. 5	K_b	Total
Gravity load, P_i (kN)	941.0	1,729	1,729	1,729	941.0	-	**7,068**
f/f_y	100.0%	100.0%	100.0%	100.0%	100.0%	-	-
Lateral Stiffness, $S_{T,i}$ (kN/m)	385.8	-236.3	-236.3	-236.3	385.8	100.0	**162.6**

In the maximum solution, all of the columns yield simultaneously. This solution is the most efficient in terms of maximizing the applied loading, since all of the columns are at their yielding capacities. As the stress in the interior columns are independent of the loads on the other columns, they are loaded until they yield, and then the exterior columns are also additionally loaded until yielding occurs in the exterior columns. The solution to the maximization problem has a total applied gravity load of 7,068 kN and corresponds to a decrease of 6.2% compared even to the more conservative inelastic analysis with instability as the constraint in variable loading (the total applied load in the maximum case in the inelastic instability analysis was 7,530 kN).

4.2.5 Effects of Increasing the Column Imperfections

In addition to the variable loading results obtained from Sections 4.2.2 through 4.2.4, the effects of varying the magnitudes of the column imperfections on the results of the corresponding

variable loading analyses was investigated. Of course, the results in Section 4.2.1 corresponding to the instability failure criterion are independent of the column imperfections. Table 10 summarizes the results obtained from the variable loading analysis corresponding to three cases: (1) $\Delta_0 = H/500$ and $\delta_0 = -H/1000$ for all columns, corresponding to the previous results; (2) $\Delta_0 = H/500$ and $\delta_0 = -H/500$ for all columns; and (3) $\Delta_0 = H/200$ and $\delta_0 = -H/200$ for all columns. From Cases 1 through 3, the values of the column imperfections become more extreme. Note that all of the analyses correspond to negative values of the out-of-straightness, δ_0. The reason for this is that upon further investigation of this example, the negative values of δ_0 correspond to the worst values of the inter-storey displacement, Δ, and deflections, δ, compared to that computed with positive δ_0 of the same magnitude.

Table 10 – Variable loading results (expressed in total loads, kN) with varying column imperfections

Criteria	$\Delta^* = H/100$		$\delta^* = H/100$		Onset of yielding	
	Min.	Max.	Min.	Max.	Min.	Max.
Case 1	2,421†	6,819	2,342	6,552	2,479	7,068
Case 2	2,421†	6,769	2,251	6,450	2,302	6,893
Case 3	2,421†	5,548	1,977	4,172	1,987	5,778

† Denotes that the scenario is governed by rotational buckling of a single interior column according to Table 2b

As demonstrated in Table 10, the loading capacities in both the minimum and maximum variable loading solutions generally decrease as the magnitudes of the column imperfections increase. In all of the columns of Table 10, the loading patterns in the solutions are common to all three cases. Note that for the minimum case corresponding to excessive inter-storey displacement (Δ^*), the rotational buckling of an interior column always occurs before the permissible inter-storey displacement is reached. Overall, it is demonstrated that an increase to the magnitude of the columns imperfections further decreases the loading capacities achieved in the variable loading analysis.

5 Conclusion

Presented in this paper is a methodology of evaluating the capacity of a steel storey frame subjected to out-of-plumbness and out-of-straightness column initial imperfections, including in variable loading. The effects of the imperfections on deflections can be represented exactly via use of the notional load concept. The proposed method also includes the use of a new notional load to account for the effect of out-of-straightness imperfections on the inter-storey displacement. To account for variable loading, a minimization problem can also be solved to determine the worst- and best-case gravity loading distributions that would cause the capacity of the frame to be reached. The capacity can be related to instability, excessive inter-storey displacement, excessive deflections, or the onset of yielding in the columns. Numerical examples are presented to compare the effects of the imperfection functions on the inter-storey displacement and maximum deflection in a frame, and to demonstrate the use of the variable loading method. The results were compared against the results of a finite element analysis and found to be accurate with the maximum difference of the frame deflection less than 1%. Based on the results of the variable loading analysis, the maximum capacity of a frame constructed according to the construction tolerances stipulated in [12] can be reduced by up to 13.0% for the given example when excessive inter-storey displacement, excessive deflections or the onset of yielding of columns are considered as failure criteria, compared to when only the stability of the frame is considered. The minimum capacity of the frame was also reduced by up to 3.3% when considering the excessive deflection criterion. It was further demonstrated that either the rotational buckling of a column in a frame or the excessive deflections occurring when column imperfections are introduced can govern its variable loading capacity. The presence of initial column imperfections at sufficient magnitudes could therefore significantly reduce the capacity of a semi-braced steel frame when the second-order effects are considered, even if it is

constructed within the permissible tolerances. The proposed method is therefore useful as a stepping stone towards the continued development of advanced structural steel analysis and design methods. It can also be extended towards multi-storey frames via decomposition into individual storeys.

ACKNOWLEDGEMENTS

The authors wish to thank the National Science and Engineering Research Council (NSERC) (RGPIN-203154-2013) of Canada for the financial support of this work.

REFERENCES

1. Schmidt, J.A. (1999). Design of Steel Columns in Unbraced Frames using Notional Loads. *Practice Periodical on Structural Design and Construction*, vol. 4, no. 1, pp. 24-28.
2. Xu, L., Wang, X. (2008). Storey-based column effective length factors with accounting for initial geometric imperfections. *Engineering Structures*, vol. 30, no. 12, pp. 3434-3444.
3. Yura, J. (1971). The effective length of columns in unbraced frames. *Engineering Journal*, vol. 8, no. 2, pp 37-42.
4. LeMessurier, W. (1977). A practical method of second order analysis Part 2 – Rigid Frames. *Engineering Journal*, vol. 14, no. 2, pp. 49-67.
5. Lui, E.M. (1992). A novel approach for K factor determination. *Engineering Journal*, vol. 29, pp. 150-159.
6. Aristizabal-Ochoa, J.D. (1997). Storey stability of braced, partially braced, and unbraced frames: classical approach. *Journal of Structural Engineering*, vol. 123, no. 6, pp. 799-807.
7. Xu, L. (2001). The buckling loads of unbraced PR frames under non-proportional loading. *Journal of Constructional Steel Research*, vol. 58, pp. 443-465.

8. Clarke, M. J., Bridge, R. Q. (1992). The inclusion of imperfections on the design of beam-columns. *Proc., 1992 Annu. Tech. Session,* Structural Stability Research Council, Bethlehem, PA, 327-346.

9. AISC. (2017). Steel construction manual, 15th edition. American Institute of Steel Construction, Chicago, IL.

10. SA. (1990). *AS4100-1990 steel structures.* Standards Australia, Sydney, Australia.

11. CEN. (1992). *ENV 1993-1-1 Eurocode 3, Design of steel structures, Part 1.1 – General rules and rules for buildings*. European Committee for Standardization, Brussels.

12. CSA. (2014). *Design of steel structures, CAN/CSA-S16-14.* Canadian Standards Association, Rexdale, Ontario, Canada.

13. Xu, L., Wang, X. (2007). Stability of multi-storey unbraced steel frames subjected to variable loading. *Journal of Constructional Steel Research*, vol. 63, pp. 1506-1514.

14. Zhuang, Y. (2013). Storey-based stability analysis of unbraced steel frames at ambient and elevated temperatures. PhD thesis, University of Waterloo.

15. Monforton, G., Wu, T. (1963). Matrix analysis of semi-rigidly connected frames. *Jouranl of the Structural Division,* vol. 89, no 6, pp. 13-42.

16. Xu, L., Liu, Y. (2002). Storey-based effective length factors for unbraced PR frames. *Engineering Journal*, vol. 39, no. 1, pp. 13-29.

17. Xu, L. (2003). A NLP approach for evaluating storey-buckling strengths of steel frames under variable loading. *Structural and Multidisciplinary Optimization,* vol. 25, no. 2, pp. 141-150.

18. Yura, J.A., Helwig, T.A. (1995). *Bracing for stability*. American Institute of Steel Construction.

19. NRC. (2015). *National Building Code of Canada 2015.* Associate Committee on the National Building Code, Ottawa, ON.

20. Ziemian, R. (2010). *Guide to Stability Design Criteria for Metal Structures, 6th ed.* Wiley & Sons Ltd.

21. Simulia, (2012). ABAQUS/CAE User's Manual (version 6.12). Dassault Systèmes Simulia Corp., Providence, RI.

22. Lasdon, L.S., Fox, R.L., Ratner, M.W. (1973). Nonlinear optimization using the generalized reduced gradient method. Case Western Reserve University, Cleveland, OH.

23. György, A., Kocsis, L. (2011). Efficient multi-start strategies for local search algorithms. *Journal of Artificial Intelligence Research,* vol. 41, no. 2011, pp. 407-444.